Propylene–Ethylene Random Copolymers: Comonomer Effects on Crystallinity and Application Properties

Markus Gahleitner,[1] Pirjo Jääskeläinen,[2] Ewa Ratajski,[3] Christian Paulik,[1] Jens Reussner,[1] Johannes Wolfschwenger,[1] Wolfgang Neißl[2]

[1]*Borealis GmbH, Innovation Center Linz, A-4021 Linz, Austria*
[2]*Borealis AS, Innovation Center Rønningen, N-3960 Stathelle, Norway*
[3]*Johannes Kepler University Linz, Institute of Chemistry, A-4040 Linz, Austria*

Received 19 February 2004; accepted 26 July 2004
DOI 10.1002/app.21308
Published online in Wiley InterScience (www.interscience.wiley.com).

ABSTRACT: For understanding the correlation chain from the polymer structure to the final application properties of propylene–ethylene random copolymers, four commercial grades with different ethylene content (0–8 mol %) but identical molecular weight distributions were investigated. Structural investigations concerning the comonomer distribution, using two different techniques (temperature rising elution fractionation and stepwise isothermal segregation), showed an increase of inhomogeneity with the total comonomer content, which was reflected for temperature rising elution fractionation in a widening of the elution temperature range. Crystallinity and crystallization speed studies confirmed the reduced overall crystallinity and increase of γ-modification content as reported previously, but they also showed the reason for these effects in the distinctive decrease of the spherulitic growth speed. Good correlations of all these parameters to the mechanical performance of the four materials were obtained. © 2005 Wiley Periodicals, Inc. J Appl Polym Sci 95: 1073–1081, 2005

Key words: polypropylene; copolymerization; fractionation of polymers; differential scanning calorimetry; crystallization; mechanical properties

INTRODUCTION

The global market position of polypropylene (PP) in comparison to other commodity thermoplastics shows a constant above-average growth of the production volume. One of the main reasons for this is the steady expansion into new application areas, in which other polymers as well as nonpolymeric materials are being substituted.[1]

Out of the PP global market volume of roughly 27,000,000 T in the year 2000, propylene–ethylene random copolymers (P/E-RACOs) have a minor but economically important share. The main application areas of P/E-RACOs are film, rigid packaging (i.e., injection molding and blow molding), and pipe applications, the proportions of which can be found in Table I.[2] The advantages of this class of polymers are improved transparency, relative softness, lower sealing temperature, and moderate low-temperature impact strength due to the lowered glass-transition temperature.

The development of new grades can be facilitated by an improved understanding of the structure–property relations governing the material behavor. This starts at the catalyst level and proceeds via polymerization and modification processes to conversion and the final material properties.[3]

Background and earlier studies

Several investigations of the composition and molecular structure of P/E-RACOs have shown the effects of catalyst and polymerization conditions on the material.[4,5] The high yield Ziegler–Natta catalyst has a tendency to concentrate stereodefects into the low molar mass chains, leading to a broad tacticity distribution and intermolecular heterogeneity of PP.[6] Ethylene units in PP–ethylene copolymers are equally concentrated in low molecular weight chains. In several crystallinity and crystallization studies[7,8] the effect of comonomer incorporation into the chains has been analyzed.

Advanced PP grades have been developed in recent years,[9] characterized mostly by improved homogeneity of the materials and the absence of low molecular weight fractions that previously deteriorated the processing behavior as well as the organoleptic properties of the materials. Especially in the case of higher ethylene contents, the homogeneity of monomer incorporation is essential for maintaining a single-phase structure.[10]

Measurement of the isotacticity distribution[11] and ethylene distribution in P/E copolymers[12] has been

Correspondence to: M. Gahleitner (markus.gahleitner@borealisgroup.com).

TABLE I
Applications of PP Resins in North America and Europe in 2000

	Europe	North America
Fiber	22	27
Film	19	12
IM/BM packaging	17	16
IM consumer	7	13
IM engineering	17	3
Other	18	29

M, injection molding; BM, blow molding; other, includes compounding and trader sales in North America. Adapted from Le Blanc et al.[2]

performed by using the temperature rising elution fractionation (TREF) technique, which fractionates polyolefins according to their solubility differences. For crystalline polymers, the solubility of the polymer chain is influenced mostly by the concentration of chain defects. It has been clearly demonstrated for PP that TREF fractionates the polymer according to the longest crystallizable sequences in the chain, which increase almost linearly with the elution temperature.[13] It is known that ethylene units act as chain defects and it is possible to achieve the desired average length of isotactic sequences by the controlled incorporation of the same.

The TREF method is very time consuming and therefore a quicker and easier method based on suitable thermal treatments in differential scanning calorimetry (DSC) has been developed. In this procedure a specimen is completely melted in order to remove all memory of its previous thermal history and then crystallized stepwise at successively lower temperatures. The heterogeneity of isotactic PP can be determined in a much shorter time using the DSC fractionation method compared to TREF and similar compositional information is obtained, although the curves are not identical. This has been used to study intermolecular heterogeneity in short-chain branched polyethylenes.[14,15] For PP, this technique has thus far been used only by Hardy et al.[16] for achieving a better separation between different crystal modifications (α/β).

The stepwise isothermal segregation technique (SIST) fractionates the material according to chain regularity (the average length of isotactic PP sequences between the defects). The isothermal crystallization at a certain temperature allows the crystallization of lamellae with a large enough dimension to be stable at that temperature. Upon isothermal crystallization at decreasing temperatures it is thus possible to fractionate the polymer in terms of lamella size. At the highest crystallization temperature only the most regular polymer chains are able to crystallize. As the temperature decreases, the critical length decreases.

The crystallization of the material plays an important role for the end-use properties of PP as for other semicrystalline polymers. Different factors have been found to influence the crystallization behavior of isotactic PP: stereoregularity,[17,18] comonomer type and content,[19] molecular weight distribution (MWD),[20,21] and heterogeneities like catalyst residues and nucleating agents.[22,23]

The ethylene units act as disturbances in the chain, hindering crystal growth and enforcing chain folding. This results not only in reduced crystallinity but also in specificities of crystal modification development.[24] In all cases, an increase of the γ modification with increasing ethylene content was found. A recent study covering very low comonomer contents[25] shows an onset of this effect already at 0.5 mol % ethylene, but it also finds strong effects from nucleation and the cooling rate. This also has consequences for the thermal behavior and the mechanical and optical properties of the material.[26]

This article is based on studies analyzing the effects of the comonomer content of P/E-RACOs on the crystallization behavior as well as the end-use properties of these materials.

EXPERIMENTAL

Materials

A homopolymer (Borealis HD244CF) and three P/E-RACOs with different ethylene contents (Borealis RD204CF, RD226CF, and RD208CF) were used in this study. All four materials are commercial resins produced in production units using bulk polymerization in liquid propylene and a fourth-generation Ziegler–Natta type catalyst with a conventional external donor. All grades have a melt flow rate (230°C/2.16 kg according to ISO 1133) of 8 g/10 min, a weight-average molecular weight (M_w) of ~310 kg/mol, and a polydispersity (M_w/M_n) of ~3.4. The latter data were determined with high-temperature size exclusion chromatography (135°C) using trichlorobenzene as a solvent.

The narrow MWD of the materials, which is advantageous in cast-film applications and thin-wall injection molding, results from a controlled degradation of the reactor product with peroxide (visbreaking or CR process[27]). The basic characteristics of all grades are presented in Table II. The glass-transition temperature (T_g) was determined with dynamic mechanical analysis in torsion (ISO 6721-2); the melting temperature (T_m), melting enthalpy (ΔH_m), and crystallization temperature (T_c) were determined with DSC (ISO 3146) using a heating and cooling rate of 10 K min^{-1}.

Structural investigations

For the determination of the total ethylene content, Fourier transform IR spectroscopy (FTIR) and NMR

TABLE II
Basic Characteristics of Investigated PP

Type	Ethylene		T_m by DSC (°C)	T_g by DMTA (°C)	Flexural modulus (MPa)	Charpy NIS (kJ/m^2)
	FTIR (wt %)	NMR (mol %)				
HD244CF	0	0	164	3	1300	3.5
RD204CF	2.2	3.4	153	−4	1000	5
RD226CF	3.4	5.2	145	−7	800	11
RD208CF	4.9	7.3	139	−10	605	14

All mechanical data are at +23°C on specimens injection molded according to ISO 1873-2; flexural modulus, ISO 178; Charpy NIS, notched impact strength ISO 179 1eA.

spectroscopy (^{13}C-NMR) were used (Fig. 1). Both methods are frequently used for the characterization of P/E copolymers, but FTIR has a significant difference from ^{13}C-NMR measurements: the latter are performed in solution[28] and therefore reflect molecular characteristics only whereas compression molded and annealed films are used for the FTIR measurements,[29] which therefore also reflect sample preparation effects and nucleation.

For the NMR measurements, the samples were dissolved in 1,2,4-trichlorobenzene and measured in a CMX 400 Infinity NMR spectrometer at 130°C.

In the FTIR measurements, films of 250-μm thickness were compression molded at 225°C and investigated on a Perkin–Elmer System 2000 FTIR instrument. For identification of the sequence distribution of the comonomer ethylene, the band range between 720 and 733 cm^{-1} must be investigated. Note especially that the band at 733 cm^{-1} indicates a random insertion and the band at 720 cm^{-1} indicates an insertion as a block sequence (more than two sequential ethylene units in the chain).

Fractionation of the PP samples was achieved by using analytical TREF. The TREF elution profiles were generated using a home-made instrument, which is similar to a published design.[30] The sample was dissolved in xylene at a concentration of 2–4 mg/mL at 130°C and injected into the column at the same tem-

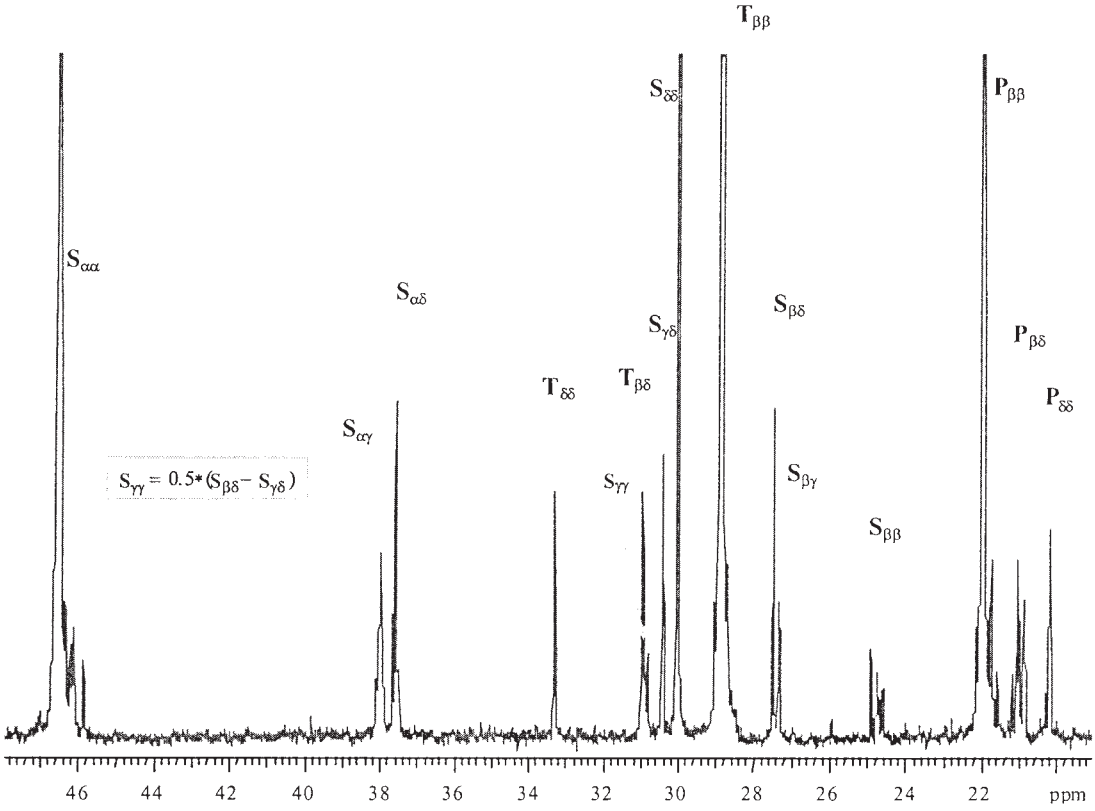

Figure 1 The peak assignment in ^{13}C-NMR of ethylene–propylene copolymers. (For details, see Di Martino and Kelchtermans.[28])

perature, and the latter was then cooled to 20°C at a rate of 1.5 K/h. The column was subsequently eluted with 1,2,4-trichlorobenzene (TCB) at a flow rate of 0.5 mL/min while the temperature was increased from 20 to 130°C over 4.5 h. The output, detected with an IR detector operating at a wavelength of 3.41 μm, was presented as a fractogram normalized to constant area.

The isothermal crystallization for SIST analysis was performed in a Mettler TA820 DSC on 3 ± 0.5 mg samples at decreasing temperatures between 145 and 105°C. The samples were melted at 225°C for 5 min, cooled at 80°C/min to 145°C for 2 h, and then cooled to the next crystallization temperature. Each of the five temperature ramps took 2 h and a step was 10°C. After the last step the sample was cooled down to ambient temperature and heated to 200°C at 10°C/min. All measurements were performed in a nitrogen atmosphere.

The melting curve of the material crystallized this way can be used for calculating the lamella thickness distribution and isotactic sequence length distribution. The longest crystallizable sequences form the thickest lamella that melt at the highest temperature because the melting temperature depends on the lamella thickness. According to the Thomson–Gibbs equation,[31] the melting temperature can be calculated as

$$T_m = T_m^0\left(1 - \frac{2\sigma}{\Delta H_0 \cdot L}\right) \quad (1)$$

where $T_m^0 = 457$ K, $\Delta H_0 = 184 \times 10^6$ J/m^3, $\sigma = 0.049.6$ J/m^2, and L is the lamella thickness. In case of the copolymers, T_m^0 has to be replaced by the respective equilibrium melting point (T_m^C).

The average isotactic sequence length distributions were calculated from the lamella thickness using a fiber length of 6.5 Å for the 3_1 helix of PP. To attain a quantitative view of the sequence length distribution in the polymer, the melting curve was divided into areas with a temperature interval of 10°.

Nucleation density and spherulitic growth rate were determined analogously to earlier studies.[17] In addition to improvements on the methodical side of the growth rate determination, a new type of thin-slice experiment was also developed for materials with very high nucleation density like externally nucleated PP grades or even high density polyethylene.

For this new method, samples of ~0.2-μm thickness were prepared by evaporating several droplets of a polymer solution in xylene placed on a microscopy cover glass at room temperature. The film thus formed was then heated after covering with a second glass to well above the melting temperature for about 30 min before cooling to room temperature. For the actual experiments, the polymer film sandwiched between cover glasses was placed in a fluid container that can be heated electrically and cooled with fluids flowing around the sample arrangement from both sides. After heating to >200°C and relaxing the sample there, it was quenched by feeding a thermostating liquid (ethylene glycol) at the crystallization temperature through the setup; the quality of this quench is illustrated by the temperature curve of Figure 2. After the selected crystallization time, the cell was flooded with water for a second chill to room temperature. The resulting samples were then analyzed in polarizing light microscopy.

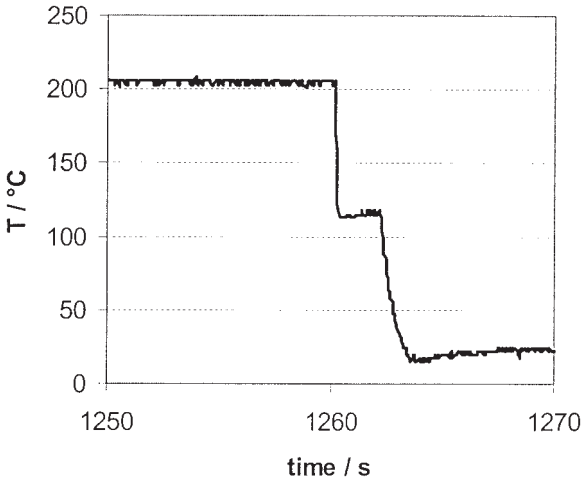

Figure 2 The temperature profile of a thin-slice experiment for determination of the growth rate (e.g., crystallization for 2 s at 115°C).

The overall crystallinity of the polymers was calculated from the density, assuming 930 kg/m^2 for pure crystalline isotactic PP,[32] and from standard DSC scans, where the problem of melting enthalpy selection exists because of conflicting literature data. For our case, a value of 209 J/g was used.[33] A wide-angle X-ray scattering (WAXS) investigation of the materials yields not only a third crystallinity value but also a determination of the γ-modification content.[34] The total crystallinity (X_c) was determined from the peak areas in the region of $10° \leq 2\theta \leq 30°$; the concentration of the α modification is expressed by the concentration parameter G [eq. (2)]. All crystallinity and crystallization data are summarized in Table III.

$$G = \frac{I_{\gamma-130}}{I_{130} + I_{\gamma-130}} \quad (2)$$

Mechanical properties

Basic mechanical data were determined on specimens injection molded according to ISO 1873-2 standard conditions (see Table II). The flexural modulus (ISO

TABLE III
Crystallization Characteristics and Crystallinity of Investigated PP

Type	X_c (%) Dens.	X_c (%) DSC	X_c (%) WAXS	γ (%)	G_c at 110°C (m/s)	N_c at 115°C ($1/m^3$)
HD244CF	55.6	49.5	40.5	0	2.05E-06	1.65E+13
RD204CF	52.1	41.3	36.2	7	1.32E-06	1.70E+13
RD226CF	47.9	36.3	ND	ND	6.58E-07	3.75E+13
RD208CF	46.7	33.9	31.6	17	5.12E-07	3.88E+13

178) and Charpy notched impact strength (ISO 179 1eA) at +23°C were determined.

Because film applications constitute a major use of this type of polymer, the mechanical parameters of 50-μm cast films were determined as well (Table IV). The generally strong influence of the processing parameters was accounted for by choosing an industrially relevant temperature for the chill roll of the cast film unit (15°C on the first roll, 25°C on the second roll; production fed with a single-screw extruder at a melt temperature of 250°C, 80-mm die width). It was demonstrated previously that the industrially used quenching of cast films with very low chill roll temperatures enforced changes in the crystallinity and mechanics over time.[35] Therefore, all data were determined after 96-h storage at +23°C.

RESULTS AND DISCUSSION

Establishing a correlation chain from the comonomer content and distribution via the crystallinity to the mechanics and optics of P/E-RACOs is a key element of the general structure–property relation for PP. This was attempted here for the class of P/E-RACOs.

Comonomer content and distribution

The two methods used for further analyzing the comonomer distribution (TREF and SIST) are considered first. As the TREF diagrams in Figure 3 already show, the comonomer addition leads not only to a decrease of the maximum elution temperature but also to a widening of the elution temperature range. This effect, which becomes more pronounced with increasing ethylene content, reflects the inhomogeneity in the way the comonomer is incorporated into the PP chains.

In the raw data of the SIST analysis (see Fig. 4), this is reflected in the depression of the melting peak as well as a progressive widening of the melting range. The lower the SIST-measured peak at the highest enthalpy derivative, the more defects there are in the polymer. It becomes even clearer when considering the isotactic sequence length distribution in Figure 5 [calculated based on eq. (1)], which effectively demonstrates the absence of longer isotactic chain segments in the random copolymers. This further affects the crystallization behavior and the final product properties. The increasingly wide melting range, which can already be seen from standard DSC scans, also determines the sealing and welding behavior of these materials and explains the technical advantage of P/E-RACOs with higher ethylene contents as functional layers enhancing the sealability.

Table V compares the peak values of standard DSC, SIST, and TREF analyses. The relation

$$T_{SIST} > T_{DSC} > T_{TREF} \quad (3)$$

TABLE IV
Cast Film Properties at +23°C

Type	Modulus (MPa)	Yield stress (MPa)	Extension at yield (%)	Penetration work (J/mm)
HD244CF	650	18	8	14
RD204CF	500	17	10	17
RD226CF	420	15	12	20
RD208CF	350	13	13	23

Tensile test in machine direction, ISO 527-3, instrumented penetration test, ISO 7765-2; 50-μm cast film (extrusion parameters, see text).

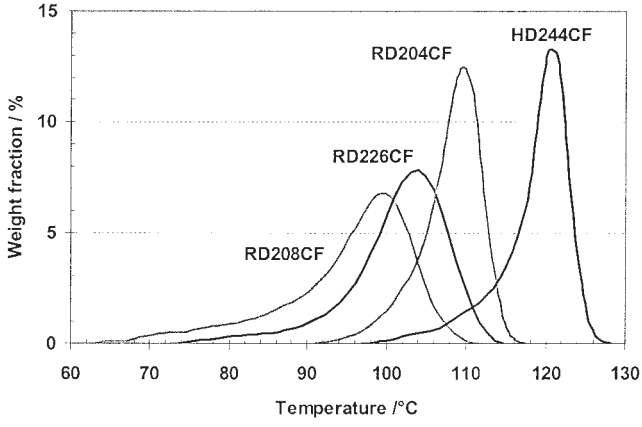

Figure 3 The TREF results of the four different polymers with TCB elution at a flow rate of 0.5 mL/min and the temperature rising from 20 to 130°C over 4.5 h.

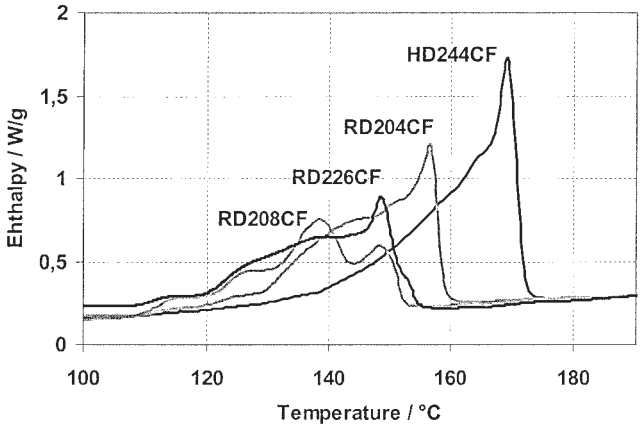

Figure 4 The raw data of the SIST analysis for the four different polymers.

is maintained throughout the whole series of materials, the difference between the two calorimetric methods being clearly attributable to an annealing effect in the SIST procedure.

Crystallinity and crystallization

The predictive power for the final properties of different structural analysis methods, for example, the different measures for crystallinity (Table IV), was previously compared for metallocene catalyst based isotactic PP.[36] The following equation can be established for relating the ethylene content (mol %) to the DSC crystallinity:

$$X_c\,(\mathrm{DSC}) = 49.024 - 2.2704E_m \qquad (4)$$

TABLE V
Correlation Between Peak Temperatures of TREF (Elution Maximum), SIST, and Standard DSC (Melting Peak)

Type	TREF (°C)	SIST (°C)	DSC (°C)
HD244CF	121	169	163
RD204CF	110	157	150
RD226CF	104	149	142
RD208CF	100	139	138

with a correlation coefficient (R^2) above 0.98. The linearity is clearly given in the comonomer concentration range under consideration.

A more complex analysis is required for understanding the effect of comonomer incorporation on the solidification process in practice. Because these processes are normally strongly nonisothermal, sometimes involving very high cooling rates, the temperature dependence of the nucleation densities (N_c) and growth rate (G_c) are required for modeling the solidification.

For both N_c and G_c very similar temperature dependences were found for all four materials (see Fig. 6). This allowed the use of one representative temperature shown in Table III. A good correlation between the ethylene content and both total X_c and spherulitic G_c was found to be possible (see Fig. 7). At the same time the effects on the N_c (see Table III) are small and possibly result from differences in the combination of processing aids and stabilizers (e.g., addition of an antiblocking agent, SiO_2).

To get an impression of the practical consequences of these differences, the evolution of the relative crys-

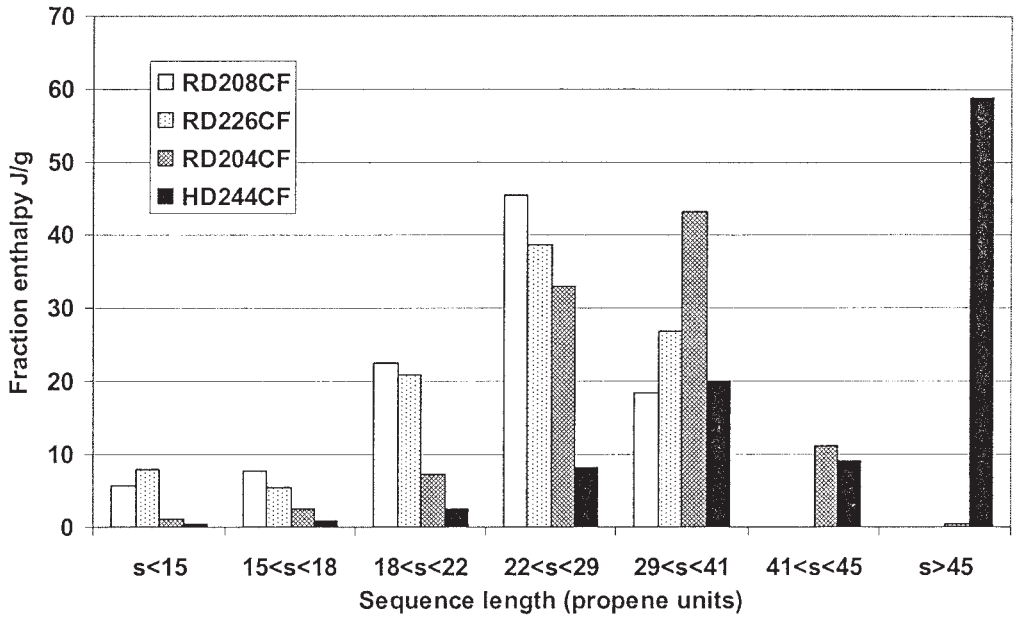

Figure 5 The sequence length distribution resulting from the SIST analysis [according to eq. (1)].

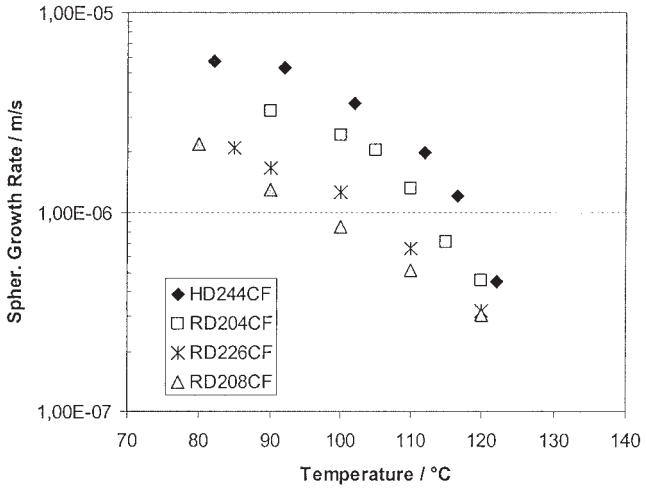

Figure 6 The temperature dependence of the spherulitic growth rate (G_c) for the four different polymers (from thin-slice experiments).

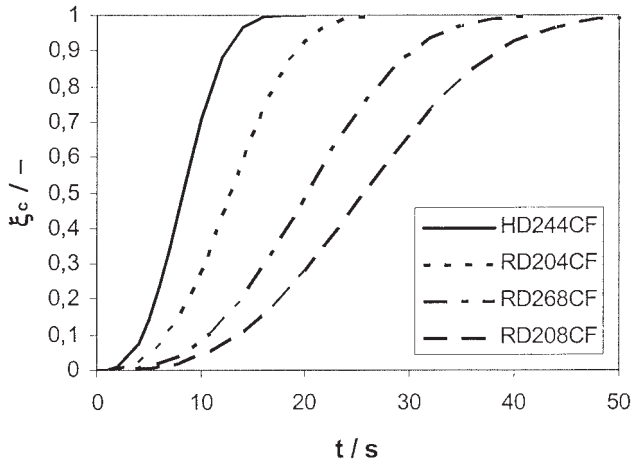

Figure 8 The predicted evolution of the relative crystallinity (ξ_c) from the nucleation density and growth rate data for the four different polymers (isothermal at 110°C).

tallinity (ξ_c) was calculated for an isothermal crystallization at 110°C in quiescent melt based on these data. With these assumptions, a combination of the Schneider rate equations as described by Eder et al.[37] leads to the following time dependence of the total crystal volume (ϕ_0):

$$\phi_0 = t^3 G_c^{\,3}(4/3\pi N_c) \tag{5}$$

In combination with the usual Avrami model for spherulitic impingement,

$$-\ln(1-\xi_c) = \phi_0 \tag{6}$$

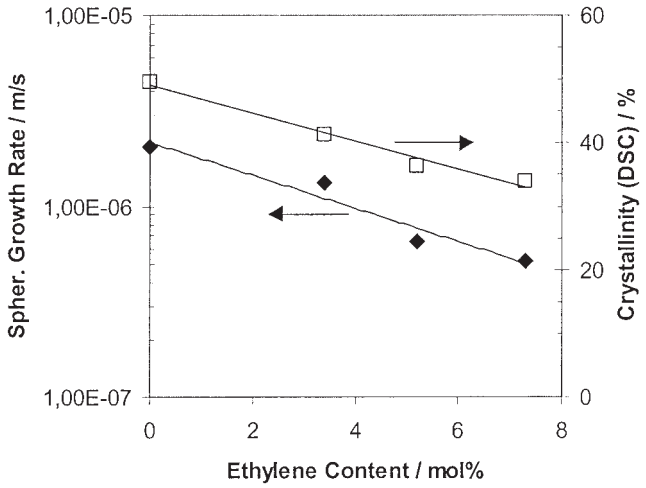

Figure 7 The influence of the ethylene content on the spherulithic growth rate (G_c; T = 110°C) and overall crystallinity calculated from the melting enthalpy (H_m) in standard DSC.

a closed formulation for $\xi_c(t)$ can be obtained. Figure 8 shows the theoretical curves for the four investigated polymers at 110°C, demonstrating the nearly fivefold increase of the time to equilibrium crystallinity for the highest ethylene content as compared with the homopolymer.

Mechanical properties

Crystallinity and modulus are roughly proportional for semicrystalline polymers. However, in practical conversion the cooling rate and, especially for injection molded parts, flow induced crystallization will play a major role in the development of both quantities. A variation of the average cooling rate[25] will affect the amount of quenching and the crystallinity level that is actually reached. More detailed studies for molding[38] and cast films[39] have demonstrated a wide variability of application properties for identical PP types.

Nevertheless, both the flexural moduli of the molded specimens and the tensile moduli of the 50-μm cast films were found to correlate nicely with the total ethylene content in the present study (see Fig. 9). In both cases, a linear correlation with the ethylene (mol %) content can be established with R^2 values above 0.99. For the flexural modulus (M_{flex}), the equation is

$$M_{\text{flex}} = 1307 - 95.9E_m \tag{7}$$

Secondary effects like flow instability in cast film extrusion, postcrystallization in conversion, or sterilization[34] are important for practical applications but less easy to understand in terms of the polymer structure. The same holds for the toughness parameters, which are additionally related to the distance between the

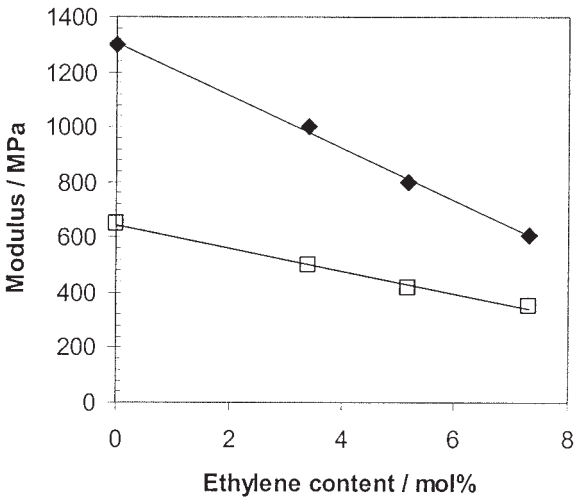

Figure 9 The correlation between the total ethylene content, (♦) flexural modulus from injection molded specimens, and (□) tensile modulus from cast film specimens.

testing temperature (+23°C) and glass-transition temperature (see Table II). Linearity can therefore not be expected, and the limited toughness increase for the cast films should probably be understood in terms of the lower crystallinity of these specimens.

A fracture mechanics study analyzing the failure behavior of an analogous series of materials was done at the Martin Luther University of Halle–Wittenberg in Merseburg,[40] in which an increasing ductile contribution was found with increasing ethylene content. Crack-tip blunting plays an important role in the toughness increase.

CONCLUSIONS

Understanding the details of the correlation chain from the polymer structure to the final application properties opens new possibilities for product design and optimization. Isotactic PPs based on single-site catalysts[17,36,41] are of special interest, because these catalysts allow not only more homogeneous incorporation of ethylene but also the effective use of α-olefines (1-alkenes) as comonomers. Such copolymers[42] are potentially very interesting in terms of an increased formation of γ modification and improved quenchability, resulting in better transparency.

In accordance with the experiences with linear low density polyethylene (again, based on TREF), improved control of the comonomer distribution over the MWD is beneficial for better design of PP copolymer properties. Multistage processes like the Borstar PP process,[43] in which the comonomer distribution and MWD design can be largely decoupled, are essential for achieving this.

The authors thank Prof. Hermann Janeschitz-Kriegl of Johannes Kepler University Linz for coordinating the basic crystallization studies, Dr. Lajos Radics of the Hungarian Academy of Sciences for the ^{13}C-NMR investigations, Prof. Peter Zipper of Karl-Franzens-University Graz for the WAXS investigations, Mrs. Raija Vainikka and Mrs. Taru Räsänen of Borealis Polymers Oy for performing the TREF and SIST analyses, and Dr. Norbert Hafner and Dipl.-Ing. Klaus Bernreitner of Borealis Linz for helpful discussions.

References

1. Colvin, M. Mod Plast 2000, June, 67.
2. Le Blanc, J.; David, D.; Duston, F. A. Dig Polym Dev Ser I: Polyolefins 2000, 96, 89.
3. Bernreitner, K.; Hammerschmid K. In Polypropylene. An A to Z Reference; Karger-Kocsis, J., Ed.; Kluwer Academic: Dordrecht, 1999; p 148.
4. Avella, M.; Martuscelli, E.; Della Volpe, G.; Segre, A.; Rossi, E.; Simonazzi, T. Makromol Chem 1986, 187, 1927.
5. Zimmermann, H. J. J Macromol Sci Phys 1993, B32, 141.
6. Paukkeri, R.; Vaananen, T.; Lehtinen, A. Polymer 1993, 34, 2488.
7. Laihonen, S.; Gedde, U. W.; Werner, P.-E.; Martinez-Salazar, J. Polymer 1997, 38, 361.
8. Laihonen, S.; Gedde, U. W.; Werner, P.-E.; Westdahl, M.; Jääskeläinen, P.; Martinez-Salazar, J. Polymer 1997, 38, 371.
9. Wolfsberger, A.; Gahleitner, M.; Niedersüß, P. In Proceedings of the Special Polyolefins '99 Conference, Houston, TX; Schotland Business Research, Skillman, NJ, 1999; p 201.
10. Seki, M.; Nakano, H.; Yamauchi, S.; Suzuki, J.; Matsushia, Y. Macromolecules 1999, 32, 3227.
11. Mingozzi, I.; Cecchin, G.; Morini, G. Int J Polym Anal Charact 1997, 3, 293.
12. Mirabella, F. M. J Liq Chromatogr 1994, 17, 3201.
13. Viville, P.; Daoust, D.; Jonas, A. M.; Nysten, B.; Legras, R.; Dupire, M.; Michel, J.; Debras, G. Polymer 2001, 42, 1953.
14. Shanks, R. A.; Amarasinghe, G. J Therm Anal Calorim 2000, 59, 471.
15. Chen, F.; Shanks, R. A.; Amarasinghe, G. Polymer 2001, 42, 4579.
16. Hardy, G.; Milburn, G. H. W.; Nyitrai, K.; Horvath, J.; Balazs, G.; Varga, J.; Shand, A. J. J Therm Anal 1989, 35, 1891.
17. Gahleitner, M.; Bachner, C.; Ratajski, E.; Rohaczek, G.; Neißl, W. J Appl Polym Sci 1999, 73, 2507.
18. van der Wal, A.; Mulder, J. J.; Gaymans, R. J. Polymer 1998, 39, 5477.
19. Williams, S. M.; Ding, Z.; Bond, E.; Spruiell, J. E. In Proceedings of SPE ANTEC '96; Society of Plastics Engineers, Brookfield, CT, 1996; p 1820.
20. Drickman, M. R. In Proceedings of SPE ANTEC '94; Society of Plastics Engineers, Brookfield, CT, 1994; p 483.
21. Gahleitner, M.; Wolfschwenger, J.; Bernreitner, K.; Neißl, W.; Bachner, C. J Appl Polym Sci 1996, 61, 649.
22. Jarus, D.; Scheibelhofer, A.; Hiltner, A.; Baer, E. J Appl Polym Sci 1996, 60, 209.
23. Shepard, T. A.; Delsorbo, C. R.; Louth, R. M.; Walborn, J. L.; Norman, D. A.; Harvey, N. G.; Spontak, R. J. J Polym Sci B: Polym Phys 1997, 35, 2617.
24. Meille, S. Macromol Symp 1995, 89, 499.
25. Foresta, T.; Piccarolo, S.; Goldbeck-Wood, G. Polymer 2001, 42, 1167.
26. Lustiger, A.; Marzinsky, C. N.; Mueller, R. R. J Polym Sci B: Polym Phys 1998, 36, 2047.
27. Hammerschmid, K.; Gahleitner, M. In Polypropylene. An A to Z Reference; Karger-Kocsis, J., Ed.; Kluwer Academic: Dordrecht, 1999; p 95.

28. Di Martino, S.; Kelchtermans, M. J Appl Polym Sci 1995, 56, 1781.
29. Andreassen, E. In Polypropylene. An A to Z Reference; Karger-Kocsis, J., Ed.; Kluwer Academic: Dordrecht, 1999; p 320.
30. Wild, L.; Blatz, C. In New Advanced Polyolefins; Chung, T. C., Ed.; Plenum: New York, 1993; p 147.
31. Gedde, U. W. Polymer Physics; Chapman & Hall: London, 1995; p 144.
32. Welsh, W. J. In Physical Properties of Polymers Handbook; Mark, J. E., Ed.; AIP: New York, 1996; p 401.
33. Brandrup, J., Immergut, E. H., Eds. Polymer Handbook, 3rd ed.; Wiley: New York, 1989; Chapter 3.
34. Weidinger, A.; Hermans, P. H. Macromol Chem 1961, 50, 98.
35. Gahleitner, M.; Fiebig, J.; Wolfschwenger, J.; Dreiling, G.; Paulik, C. J Macromol Sci Phys 2002, B41, 833.
36. Isasi, J. R.; Mandelkern, L.; Galante, M. J.; Alamo, R. G. J Polym Sci B: Polym Phys 1999, 37, 323.
37. Eder, G.; Janeschitz-Kriegl, H.; Liedauer, S. Prog Polym Sci 1990, 15, 629.
38. Phillips, R.; Herbert, G.; News, J.; Wolkowicz, M. Polym Eng Sci 1994, 34, 1731.
39. Macauley, N. J.; Harkin-Jones, E. M. A.; Murphy, W. R. Polym Eng Sci 1998, 38, 662.
40. Fierment, U. Ph.D. Dissertation, Martin Luther University of Halle–Wittenberg, Merseburg, Germany, 1994.
41. Fischer D.; Mühlhaupt, R. Macromol Chem Phys 1994, 195, 1433.
42. Pérez, E.; Zucchi, D.; Sacchi, M. C.; Forlini, F.; Bello, A. Polymer 1999, 40, 675.
43. Grande, H. M. In Proceedings of the Polypropylene '99 Conference, Zürich; Maack Business Services, Zürich, CH, 1999; p 1.